

## Atmospheric mercury outflow from China and interprovincial trade

Long Chen, Sai Liang, Yanxu Zhang, Maodian Liu, Jing Meng, Haoran Zhang,  
Xi Tang, Yumeng Li, Yindong Tong, Wei Zhang, Xuejun Wang, and Jiong Shu

*Environ. Sci. Technol.*, **Just Accepted Manuscript** • DOI: 10.1021/acs.est.8b03951 • Publication Date (Web): 29 Oct 2018

Downloaded from <http://pubs.acs.org> on October 30, 2018

### Just Accepted

“Just Accepted” manuscripts have been peer-reviewed and accepted for publication. They are posted online prior to technical editing, formatting for publication and author proofing. The American Chemical Society provides “Just Accepted” as a service to the research community to expedite the dissemination of scientific material as soon as possible after acceptance. “Just Accepted” manuscripts appear in full in PDF format accompanied by an HTML abstract. “Just Accepted” manuscripts have been fully peer reviewed, but should not be considered the official version of record. They are citable by the Digital Object Identifier (DOI®). “Just Accepted” is an optional service offered to authors. Therefore, the “Just Accepted” Web site may not include all articles that will be published in the journal. After a manuscript is technically edited and formatted, it will be removed from the “Just Accepted” Web site and published as an ASAP article. Note that technical editing may introduce minor changes to the manuscript text and/or graphics which could affect content, and all legal disclaimers and ethical guidelines that apply to the journal pertain. ACS cannot be held responsible for errors or consequences arising from the use of information contained in these “Just Accepted” manuscripts.

1 **Atmospheric mercury outflow from China and interprovincial trade**

2

3 Long Chen<sup>1,2</sup>, Sai Liang<sup>3</sup>, Yanxu Zhang<sup>4</sup>, Maodian Liu<sup>5</sup>, Jing Meng<sup>6</sup>, Haoran Zhang<sup>5</sup>, Xi

4 Tang<sup>1,2</sup>, Yumeng Li<sup>3</sup>, Yindong Tong<sup>7</sup>, Wei Zhang<sup>8</sup>, Xuejun Wang<sup>5,\*</sup> and Jiong Shu<sup>1,2,\*</sup>

5

6 <sup>1</sup> Key Laboratory of Geographic Information Science (Ministry of Education), East China

7 Normal University, Shanghai, 200241, China

8 <sup>2</sup> School of Geographic Sciences, East China Normal University, Shanghai, 200241,

9 China

10 <sup>3</sup> State Key Joint Laboratory of Environment Simulation and Pollution Control, School of

11 Environment, Beijing Normal University, Beijing, 100875, China

12 <sup>4</sup> School of Atmospheric Sciences, Nanjing University, Nanjing, Jiangsu, 210023, China

13 <sup>5</sup> Ministry of Education Laboratory of Earth Surface Process, College of Urban and

14 Environmental Sciences, Peking University, Beijing, 100871, China

15 <sup>6</sup> Department of Politics and International Studies, University of Cambridge, Cambridge

16 CB3 9DT, UK

17 <sup>7</sup> School of Environmental Science and Engineering, Tianjin University, Tianjin 300072,

18 China

19 <sup>8</sup> School of Environment and Natural Resources, Renmin University of China, Beijing,

20 100872, China

**21 Abstract**

22 Mercury (Hg) is characterized by the ability to migrate between continents and adverse  
23 effects on human health, arousing great concerns around the world. The transboundary  
24 transport of large anthropogenic Hg emissions from China has attracted particular  
25 attention, especially from neighboring countries. Here, we combine an atmospheric  
26 transport model, a mass budget analysis, and a multiregional input-output model to  
27 simulate the atmospheric Hg outflow from China and investigate the impacts of Chinese  
28 interprovincial trade on the outflow. The results show outflows of 423.0 Mg of  
29 anthropogenic Hg, consisting of 65.9% of the total Chinese anthropogenic emissions,  
30 from China in 2010. Chinese interprovincial trade promotes the transfer of atmospheric  
31 outflow from the eastern terrestrial boundary ( $-6.4 \text{ Mg year}^{-1}$ ) to western terrestrial  
32 boundary ( $+4.5 \text{ Mg year}^{-1}$ ) and a net decrease in the atmospheric outflow for the whole  
33 boundary, reducing the chance of risks to foreign countries derived from transboundary  
34 Hg pollution from China. These impacts of interprovincial trade will be amplified due to  
35 the expected strengthened interprovincial trade in the future. The synergistic promotional  
36 effects of interprovincial trade versus Hg controls should be considered for reducing the  
37 transboundary Hg pollution from China.

## 38 1. Introduction

39 Mercury (Hg) is a global toxic pollutant that is characterized by long distance  
40 atmospheric transport, which contributes to its ability to migrate across the oceans  
41 between continents.<sup>1,2</sup> Owing to dry and wet scavenging, Hg can be deposited in  
42 terrestrial and aquatic ecosystems. Methylmercury (MeHg) can be formed via the  
43 methylation and bioaccumulation of Hg in food webs after deposition, adversely affecting  
44 human health, such as by causing neurocognitive deficits in children and cardiovascular  
45 problems in adults.<sup>3-7</sup> Several human health disasters have already occurred owing to  
46 MeHg exposure (e.g., Minamata disease),<sup>8</sup> promoting the launch of the *Minamata*  
47 *Convention on Mercury*.<sup>9</sup> The convention focuses on transboundary Hg pollution and  
48 controls around the world.

49 China is the largest Hg emitter in the world, releasing approximately 33% of the  
50 global total anthropogenic emissions to the air each year.<sup>1,10,11</sup> The transboundary  
51 transport of large Hg emissions outside China have aroused great concerns from all  
52 countries of the world, especially neighboring countries. For instance, combining  
53 monitoring data and meteorological data, scholars suggested that high Hg concentrations  
54 observed at Mt. Fuji and Cape Hedo in Japan might be related to the transboundary  
55 transport of Hg from China.<sup>12,13,14,15</sup> These concerns require studies focusing on  
56 atmospheric Hg outflows from China and the subsequent impacts on neighboring regions.  
57 Previous studies have illustrated that anthropogenic emissions from East Asia  
58 significantly contribute to Hg deposition over the rest of the world. For instance, 70–75%  
59 of the total emissions from East Asia were transported outside the region, and the  
60 maximum occurred in spring and early summer, contributing 20–30% of the total

61 atmospheric deposition over remote regions.<sup>16,17</sup> Anthropogenic emissions from East Asia  
62 were the primary sources for deposition over global oceans,<sup>2,18</sup> especially the Arctic.<sup>19,20</sup>  
63 However, atmospheric Hg outflows from China and the associated impacts on  
64 neighboring deposition have not been investigated.

65 China is a vast country with substantial disparities in socioeconomic development  
66 across provinces, such as in the consumption of resources and energy, population growth,  
67 and lifestyles, resulting in frequent and substantial interprovincial trade. Interprovincial  
68 trade separates production activities and final consumption and subsequently induces  
69 embodied air, water and soil pollution.<sup>21-24</sup> The atmospheric Hg emissions embodied in  
70 interprovincial trade have been well-documented in China, resulting in a comprehensive  
71 virtual atmospheric Hg emission network among Chinese provinces.<sup>25-27</sup> The network  
72 shows that a large amount of Hg emitted from inland provinces is caused by the final  
73 consumption in coastal provinces.<sup>25,26</sup> In addition to Hg emissions, previous studies also  
74 found that 32% of atmospheric deposition over China was embodied in interregional  
75 trade and that deposition was considerably redistributed by this trade.<sup>28</sup> Considerable  
76 impacts of interprovincial trade on atmospheric Hg emissions and deposition within  
77 China have been verified by previous studies, but impacts of interprovincial trade on Hg  
78 transport outside China are poorly understood.

79 In this study, we combine an atmospheric transport model, a mass budget analysis,  
80 and a multiregional input-output model to simulate the atmospheric outflow of  
81 anthropogenic Hg emitted from human activities in China and subsequent deposition over  
82 neighboring seas and lands and investigate the impacts of Chinese interprovincial trade  
83 on Hg outflow and deposition. Accordingly, suggestions on controlling transboundary Hg

84 pollution from China are proposed. The findings in our study are relevant to efforts on  
85 international collaboration to reduce transboundary Hg pollution.

86

## 87 **2. Materials and Methods**

### 88 **2.1. Study area and associated anthropogenic emissions**

89 The study domain is located from 70°E to 150°E and 11°S to 55°N, which represents  
90 the East Asian domain. This area covers China and other parts of East Asia, such as Japan,  
91 the Republic of Korea, India, Indonesia, Vietnam, Thailand, and Mongolia (Figure S1).  
92 To evaluate the impacts of interprovincial trade on foreign deposition, we choose several  
93 representative neighboring seas and lands that border on terrestrial China or that are  
94 located offshore and classify these regions into five groups according to their locations,  
95 namely, the Chinese coastal seas, Japan-Korea, Southeast Asia, South Asia, and  
96 Mongolia (*SI Dataset S1*; Figure S1). To evaluate the impacts of interprovincial trade on  
97 atmospheric outflow, we divide the whole geographic boundary of China into the eastern  
98 terrestrial boundary and western terrestrial boundary. The eastern terrestrial boundary  
99 includes all the coastlines and national boundaries located in the northeast provinces.  
100 (Figure S1).

101 Human activities, such as coal combustion, nonferrous metal smelting and cement  
102 production, emit large quantities of Hg to the atmosphere each year. In this study,  
103 anthropogenic emissions from China from the producer perspective (i.e., production-  
104 based emissions) are referenced from our previous work,<sup>28</sup> which compiled a Chinese  
105 emission inventory in 2010 by multiplying energy usage and product yields by the  
106 respective emission factors. The anthropogenic emissions are distributed as point and

107 nonpoint sources in terms of industrial productivity and gridded population density.  
108 Seasonal variations have not been evaluated for the emissions due to data unavailability.  
109 The production-based emissions for each province and each economic sector are given in  
110 *SI Dataset S4* and *Dataset S5*, respectively. Anthropogenic emissions from other parts of  
111 Asia are referenced from the AMAP/UNEP (Arctic Monitoring and Assessment  
112 Programme/United Nations Environment Programme) global anthropogenic emission  
113 inventory in 2010.<sup>1</sup>

114

## 115 **2.2. Evaluation of trade-induced emissions**

116 The calculation of the interprovincial trade-induced Hg emissions is based on an  
117 environmentally extended multiregional input-output (EE-MRIO) analysis of the  
118 interactions between different economic sectors (*SI Dataset S2*) and provinces in China  
119 multiplied by sector-specific emission intensities. The MRIO table of China in 2010  
120 developed by Liu et al.<sup>29</sup> is used in this study to evaluate interprovincial trade-embodied  
121 Hg emissions among Chinese provinces. A brief introduction of the MRIO approach is  
122 shown as follows:

$$123 \quad \mathbf{X} = (\mathbf{I} - \mathbf{A})^{-1}\mathbf{Y} \quad (1)$$

124 where  $\mathbf{X}$  is a vector of the total monetary output for different sectors,  $\mathbf{Y}$  is a vector of  
125 final demand for different sectors, including final consumption ( $\mathbf{F}$ ) (i.e., urban household  
126 consumption, rural household consumption, government consumption and investment)  
127 and international export ( $\mathbf{E}$ ).  $\mathbf{I}$  represents the unsity matrix, and  $\mathbf{A}$  denotes the direct  
128 requirement coefficient matrix. Element  $a_{ij}$  in matrix  $\mathbf{A}$  is defined as the intermediate

129 input from sector  $i$  to the production of a unit output for sector  $j$ .  $(\mathbf{I} - \mathbf{A})^{-1}$  is the *Leontief*  
130 *inverse matrix*, which is the foundation of the MRIO approach.

131 Multiplying by the direct emission intensity vector ( $\psi$ ) for equation (1), we calculate  
132 sector- and province-specific consumption-based emissions with the corresponding final  
133 consumption  $\mathbf{F}$ . We define  $\psi_0$  as a vector with zero for a given sector or province but the  
134 direct emission intensity for other sectors or provinces. Through multiplying by the  
135 vector, we calculate emissions embodied in imports (EEI) for the given sector or province  
136 with its corresponding final consumption  $\mathbf{F}$  (eq 2). The hats over  $\psi_0$  and  $\mathbf{F}$  mean  
137 diagonalizing vectors of  $\psi_0$  and  $\mathbf{F}$ . The correspondence relationships between direct  
138 emission sources and sectors of the Chinese MRIO table are shown in *SI Dataset S3*.

$$139 \quad \text{EEI} = \hat{\psi}_0 (\mathbf{I} - \mathbf{A})^{-1} \hat{\mathbf{F}} \quad (2)$$

140 To evaluate the impacts of interprovincial trade, we set up a hypothetical scenario  
141 with an absence of interprovincial trade. We assume the trade partners could produce the  
142 same goods which are originally involved in interprovincial trade locally, and then EEI of  
143 a given province are assumed to be relocated from its trade partners to the province.  
144 Similar to previous studies,<sup>30,31</sup> the assumed relocation of EEI reveals the same  
145 technologies when producing the same goods between trade partners and is used to  
146 evaluate the difference between existence and absence of interprovincial trade. The  
147 results of trade-induced emissions are shown in *SI Dataset S4* and *Dataset S5*. Meanwhile,  
148 the net emission flows induced by interprovincial trade is shown in Figure S2.

149

### 150 **2.3. Simulation of atmospheric Hg outflow and deposition**



151 The GEOS-Chem chemical transport model (version 9-02; <http://geos-chem.org>) is  
152 used to simulate atmospheric Hg deposition over the study area and atmospheric Hg  
153 outflow from China. The model is a 3-D atmosphere model that is integrated to a 2-D  
154 surface slab ocean and a 2-D soil reservoir for Hg cycle.<sup>32-34</sup> Three Hg species, namely,  
155 elemental Hg ( $\text{Hg}^0$ ), divalent Hg ( $\text{Hg}^{\text{II}}$ ) and particulate Hg ( $\text{Hg}^{\text{P}}$ ), are tracked in the model.  
156  $\text{Hg}^0$  can be oxidized to  $\text{Hg}^{\text{II}}$  by Br atoms, while  $\text{Hg}^{\text{II}}$  can be reduced to  $\text{Hg}^0$  under light in  
157 cloud droplets.<sup>33</sup> Meanwhile, the balance of gas-particle partitioning is maintained  
158 between  $\text{Hg}^{\text{II}}$  and  $\text{Hg}^{\text{P}}$ .<sup>35</sup> Dry deposition and wet scavenging of atmospheric Hg in the  
159 model follow the resistance-in-series scheme from Wesely<sup>36</sup> and the scheme from Liu et  
160 al.,<sup>37</sup> respectively. The model is driven by the assimilated meteorological fields from the  
161 Goddard Earth Observing System (GEOS-5) conducted by the NASA Global Modeling  
162 and Assimilation Office (GMAO).

163 Using the method presented in our previous work,<sup>28</sup> a nested model can be conducted  
164 over East Asia at native horizontal resolution of  $1/2^\circ \times 2/3^\circ$  and 47 vertical levels from  
165 the surface to 0.01 hPa. Before performing the nested simulation, a global  $4^\circ \times 4.5^\circ$   
166 resolution simulation is conducted first for lateral boundary conditions of the nested simulation. The  
167 global simulation is driven by emissions combining the Chinese emission inventory in  
168 China and the AMAP/UNEP global anthropogenic emission inventory outside China.<sup>1</sup>  
169 The nested model's performance has been evaluated against a series of observations in  
170 our previous work. In this study, we run the nested model with two emission scenarios  
171 representing existence and absence of interprovincial trade, respectively, in 2010 under  
172 an initial spin-up of the last three months in 2009. The lateral boundary conditions are provided by

173 global simulations during 2008–2010. The outputs are archived monthly and are used to illustrate  
174 seasonal variations in atmospheric outflow and deposition.

175

#### 176 **2.4. Calculation of regional Hg mass budget**

177 The atmospheric Hg outflow from China is estimated by calculating Hg mass budget  
178 for China using the GEOS-Chem simulation results for each modeling month. We use a  
179 schematic for the regional mass budget calculation proposed by Lin et al.<sup>16</sup> In general, the  
180 change in atmospheric Hg burden within a region over a simulation period can be  
181 influenced by the Hg mass entering and leaving the region via atmospheric transport,  
182 atmospheric Hg emissions, and atmospheric Hg deposition via dry and wet scavenging.  
183 Meanwhile, the net change in atmospheric Hg burden within a region also equals the  
184 difference between the atmospheric Hg burden at the beginning and at the end of the  
185 simulation period. The schematic can be expressed by the following equations:

$$186 \quad \text{FB} - \text{IB} = \text{IM} - \text{OM} + \text{E} - \text{D} \quad (3)$$

$$187 \quad \text{OF} = \text{OM} - \text{IM} = \text{E} - \text{D} - \text{FB} + \text{IB} \quad (4)$$

188 where FB is the atmospheric burden within the region at the end of the simulation period  
189 and IB is the atmospheric burden within the region at the beginning of the simulation  
190 period. IM, OM, E and D represent the Hg mass that enters the region, the Hg mass that  
191 leaves the region, the atmospheric emissions in the region and the atmospheric deposition  
192 in the region over the simulation period, respectively. OF represents the net atmospheric  
193 outflow from the region via atmospheric transport, which can be defined as the difference  
194 between the Hg mass leaving the region and entering the region. All the terms are in Mg  
195 per period. In this study, we evaluate all the terms driven by Chinese anthropogenic

196 emissions to illustrate the impacts of human activities in terrestrial China on neighboring  
197 seas and lands.

198

### 199 **3. Results and Discussion**

#### 200 **3.1 Atmospheric Hg outflow from China**

201 In 2010, human activities in China totally release 641.7 Mg Hg to the air, 218.7 Mg  
202 of which is deposited in terrestrial China and 423.0 Mg of which is transported outside  
203 terrestrial China (Figure 1). The atmospheric outflow consists of 65.9% of the total  
204 Chinese anthropogenic emissions, and the large contribution indicates that China serves  
205 as both an important Hg emitter and an important Hg exporter globally. For the whole  
206 year, the atmospheric burden over China driven by Chinese anthropogenic emissions  
207 remains nearly constant.

208 Moreover, seasonal variations are observed for atmospheric Hg deposition and  
209 outflow for China (Figure 1b). In summer months, large near-source deposition occurs in  
210 China due to the large amount of rain, which increases atmospheric deposition over  
211 terrestrial China and subsequently reduces atmospheric outflow from terrestrial China.  
212 The largest deposition ( $24.2 \text{ Mg month}^{-1}$ ) and smallest outflow ( $27.7 \text{ Mg month}^{-1}$ ) occur  
213 in August. In winter months, in contrast, the atmospheric deposition over terrestrial China  
214 decreases and atmospheric outflow increases subsequently due to lower amount of rain  
215 and limited scavenging in winter in China. The smallest deposition ( $13.1 \text{ Mg month}^{-1}$ )  
216 and largest outflow ( $41.4 \text{ Mg month}^{-1}$ ) values occur in February. The seasonal difference  
217 reveals that human activities in China contribute more to domestic Hg pollution in  
218 summer months and neighboring Hg pollution in winter months.

219

**220 3.2 Impacts of interprovincial trade on the atmospheric outflow**

221 Human activities in China release a total of 641.7 Mg Hg to the air in 2010, 503.0  
222 Mg Hg of which is related to the final consumption of the Chinese population (*SI Dataset*  
223 *S4*). The remaining mass is related to non-economic activities (i.e., residential coal  
224 consumption and the use of Hg-added products) and foreign consumption. For a specific  
225 province in China, the final consumption includes consumption of local goods and  
226 imported goods, inducing local emissions (i.e., on-site emissions embodied in the own  
227 consumption of the province) and emissions in other provinces that are involved in  
228 interprovincial trade (i.e., EEI), respectively. For the whole nation, the imports of goods  
229 and services induce 227.6 Mg year<sup>-1</sup> Hg emissions. Meanwhile, among the EEI, 85.6 Mg  
230 year<sup>-1</sup> Hg is embodied in net interprovincial trade, which represents the net transfer from  
231 embodied Hg importers to embodied Hg exporters within China (*SI Dataset S4*).

232 Figure 2 illustrates the impacts of interprovincial trade on the net atmospheric Hg  
233 outflow from the whole boundary of China. Due to Chinese interprovincial trade,  
234 approximately 1.9 Mg year<sup>-1</sup> of net Hg would have been transported outside China, but it  
235 is deposited in terrestrial China (1.6 Mg year<sup>-1</sup>) and stored in the atmosphere (0.3 Mg  
236 year<sup>-1</sup>). Most of the embodied Hg importers are developed provinces in China located on  
237 the southeast coast, while most of the embodied Hg exporters are developing provinces in  
238 China located in inland regions. As a result of interprovincial trade, emissions flow from  
239 the southeast coast to inland regions (Figure S2), which was also reported by previous  
240 studies.<sup>26,28</sup> These emissions are easily deposited in terrestrial ecosystems and stored in

241 the atmosphere over terrestrial China due to the greater distance from the terrestrial  
242 boundaries.

243 Compared to the small net change for the whole boundary, interprovincial trade  
244 contributes more to the change in spillover channels. The emission flows from the  
245 southeast coast to inland regions during interprovincial trade contribute to the decrease in  
246 spillover from the eastern terrestrial boundary and the increase from the western  
247 terrestrial boundary (Figure 3). The decrease from the eastern terrestrial boundary is  
248 estimated to be  $-6.4 \text{ Mg year}^{-1}$  consisting of 7.5% of the emissions embodied in net  
249 interprovincial trade, while the increase from the western terrestrial boundary is estimated  
250 to be  $+4.5 \text{ Mg year}^{-1}$ . The decrease in spillover from the eastern terrestrial boundary  
251 contributes to the decrease in atmospheric deposition over the seas and lands leaving the  
252 eastern terrestrial boundary, such as the Chinese coastal seas, the Sea of Japan, Japan-  
253 Korea, and some regions in Southeast Asia (Figure 3). However, the increase in spillover  
254 from the western terrestrial boundary contributes to the increase in atmospheric  
255 deposition over the lands outside the western terrestrial boundary, such as Mongolia,  
256 South Asia, and some regions in Southeast Asia (Figure 3).

257 The transfer of atmospheric outflow from the eastern terrestrial boundary to western  
258 terrestrial boundary is a highly significant change in transboundary Hg pollution from  
259 China. As we know, human MeHg exposure stems almost entirely from the consumption  
260 of seafood, such as fish and shellfish harvested from marine regions.<sup>38-40</sup> Thus, marine  
261 regions are the critical receptors of Hg posing health risks to human beings.<sup>3,41,42</sup>  
262 Accordingly, the decrease in atmospheric outflow from the eastern terrestrial boundary  
263 and the subsequent decrease in atmospheric deposition over the seas outside the eastern

264 terrestrial boundary may reduce the Hg in seafood harvested from the seas, which can  
265 reduce the MeHg exposure risks for humans who rely heavily on marine-based diets,  
266 such as the populations of Japan and the Republic of Korea. In general, through the  
267 transfer of atmospheric outflow between different boundaries, interprovincial trade  
268 reduces the chance of risks to foreign countries derived from transboundary Hg pollution  
269 from China.

270 Moreover, the transfer of atmospheric outflow from the eastern terrestrial boundary  
271 to western terrestrial boundary is characterized by significant seasonal differences (Figure  
272 3). The seasonal differences are attributed to the prevailing wind directions of the East  
273 Asian Monsoon (Figure S3). In the autumn and winter months, seasonal winds from  
274 Siberia to the Northwest Pacific bring atmospheric Hg from the southeast coast of China  
275 to the downwind seas outside the eastern terrestrial boundary, and the decrease in  
276 deposition occurs over the seas due to exported emissions outside the southeast coast of  
277 China (Figure S3a and S3d). Meanwhile, the seasonal winds also bring atmospheric Hg  
278 from southwest China to downwind regions in South Asia, and the increase in deposition  
279 occurs over these regions due to imported emissions into southwest China (*SI Dataset S4*;  
280 Figure S2). An increase in deposition is observed over the sea and land near southern  
281 Japan during interprovincial trade, which is attributed to both imported emissions into the  
282 North China Plain (e.g., Hebei, Shandong) (*SI Dataset S4*) and the seasonal winds of the  
283 East Asian Monsoon. Meanwhile, wind shear over the region may contribute to greater  
284 deposition and amplify the increase (Figure S3a and S3d).

285 In the spring and summer months, the prevailing wind direction is from the  
286 Northwest Pacific to Siberia, the opposite direction of the wind in the autumn and winter

287 months (Figure S3b and S3c). The seasonal winds bring atmospheric Hg from inland  
288 China (e.g., Henan, Gansu, Shaanxi, and Inner Mongolia) to downwind regions outside  
289 the western terrestrial boundary, such as Mongolia. An increase in deposition occurs over  
290 these downwind regions due to the imported emissions in inland China during  
291 interprovincial trade (*SI Dataset S4*; Figure S2). Due to the seasonal winds, the decrease  
292 in atmospheric outflow from the eastern terrestrial boundary of China in the spring and  
293 summer months is weaker than that in autumn and winter months. This phenomenon  
294 indicates that interprovincial trade reduces the Hg risks to foreign countries mainly in the  
295 autumn and winter months. Finally, a decrease in deposition is found along the line of the  
296 Yellow Sea, the Korean Peninsula, the Sea of Japan and northern Japan all the year round.  
297 The westerlies of the Northern Hemisphere throughout the year may contribute to this  
298 phenomenon, resulting in these regions as the most important regions benefitting from  
299 Chinese interprovincial trade.

300

### 301 **3.3 Projected impacts of interprovincial trade**

302 A large potential impact of Chinese interprovincial trade on the changes of  
303 atmospheric Hg outflow can be inferred. At present, the relocation of emissions  
304 embodied in the net interprovincial trade (85.6 Mg year<sup>-1</sup>) results in the transfer of  
305 atmospheric outflow from the eastern terrestrial boundary to western terrestrial boundary  
306 and a net decrease in the atmospheric outflow from the whole boundary. Subsequently,  
307 atmospheric deposition of Chinese anthropogenic Hg decreases over neighboring seas  
308 and lands outside the eastern terrestrial boundary, for example, -10.5% for Chinese  
309 coastal seas and -2.2% for Japan-Korea, and increases over neighboring lands outside the

310 western terrestrial boundary (Figure 4). These changes in outflow and deposition can be  
311 amplified with an increase in net interprovincial trade.

312 In addition to the emissions embodied in net interprovincial trade, the trade induces  
313 another 142.0 Mg year<sup>-1</sup> of Hg emissions that is offset due to trade balance (Figure 4).  
314 Meanwhile, the consumption of local goods by the national population also induces 275.4  
315 Mg year<sup>-1</sup> of Hg emissions that are not involved in interprovincial trade (*SI Dataset S4*;  
316 Figure 4). If the interprovincial trade is strengthened in the future, the original trade  
317 balance would be broken and the consumption of local goods would be transferred to the  
318 consumption of imported goods. Then, the emissions embodied in net interprovincial  
319 trade would become larger, which would further promote the transfer of atmospheric  
320 outflow from the eastern terrestrial boundary to western terrestrial boundary and a net  
321 decrease in the atmospheric outflow from the whole boundary given the premise of  
322 constant total anthropogenic emissions. This change will further reduce the MeHg  
323 exposure risks to humans who live in the regions outside the eastern terrestrial boundary  
324 of China and those who rely heavily on the marine-based diets. For instance, Japan-Korea  
325 totally receives 6.3 Mg year<sup>-1</sup> Hg from Chinese anthropogenic emissions. If the decrease  
326 responded proportionally to the increase of net interprovincial trade from 85.6 Mg year<sup>-1</sup>  
327 to 503.0 Mg year<sup>-1</sup>, we would expect a decrease of Chinese anthropogenic Hg from 6.3  
328 Mg year<sup>-1</sup> to 5.5 Mg year<sup>-1</sup> deposited in Japan-Korea. That is, the maximum for  
329 transboundary impacts of China on Japan-Korea can be reduced by 11%, which is  
330 equivalent to the emission ratios of some critical emission sectors in China (e.g., coal-  
331 fired power plants). In general, a further reduction in transboundary Hg pollution from  
332 China is projected with the increase in net interprovincial trade.



333

**334 3.4 Policy implications of transboundary Hg controls**

335 Policies on Chinese anthropogenic sources would contribute considerably to the  
336 mitigation of Hg-related health risks in Chinese neighboring regions in consideration of  
337 the considerable atmospheric Hg outflow. The mitigation would vary between seasons,  
338 with more mitigation occurring in the winter months due to the larger atmospheric Hg  
339 outflow in those months. Chinese interprovincial trade promotes the transfer of  
340 atmospheric outflow from the eastern terrestrial boundary to western terrestrial boundary,  
341 and a net decrease in the atmospheric outflow from the whole boundary and increase in  
342 the atmospheric deposition over terrestrial China. The decrease in deposition over  
343 neighboring regions outside the eastern terrestrial boundary is more remarkable in the  
344 autumn and winter months. Rapid industrialization and urbanization have substantially  
345 increased the consumption of goods and services and associated interprovincial trade in  
346 the past decades in China.<sup>25</sup> This change reveals that a considerable portion of Hg from  
347 Chinese human activities has not been transported outside the eastern terrestrial boundary  
348 and has been deposited in terrestrial China or transported outside the western terrestrial  
349 boundary due to increasing interprovincial trade in the past decades. Chinese  
350 interprovincial trade, to some extent, has offset the adverse effects of increasing  
351 anthropogenic Hg emissions from China on neighboring seas and lands outside the  
352 eastern terrestrial boundary of China.

353 Since the 11<sup>th</sup> Five-Year Plan, the Chinese government has committed to build and  
354 develop urban agglomerations, which calls for more domestic consumption and domestic  
355 imports. More domestic consumption and imports promote more emissions embodied in

356 interprovincial trade, which will flow from coastal developed urban agglomerations to  
357 inland developing regions in the future. The projected increase in interprovincial trade is  
358 expected to promote the transfer of atmospheric outflow from the eastern terrestrial  
359 boundary to western terrestrial boundary and the further reduction in transboundary Hg  
360 pollution from China. Alongside with the Hg controls implemented in China,  
361 interprovincial trade has a synergistic promotional effect on the reduction in atmospheric  
362 outflow, especially for the reduction in atmospheric deposition over regions outside the  
363 eastern terrestrial boundary of China. Thus, the combination of Hg controls and  
364 interprovincial trade could be considered to reduce the transboundary Hg pollution from  
365 China.

366

### 367 **3.5 Uncertainties and recommendations**

368 Our model results are subject to uncertainties from various sources, including the  
369 compilation of production-based emissions, the calculation of trade-induced emissions,  
370 and the simulation of the atmospheric chemical transport model. Since the production-  
371 based anthropogenic emissions from China are referenced from our previous work,<sup>28</sup> an  
372 overall uncertainty of [-25.0%, 29.0%] from that study is used in this study. These  
373 uncertainties are derived from knowledge gaps on Hg concentrations in fuel/raw  
374 materials, Hg removal efficiencies and activity rates. The calculation of trade-induced  
375 emissions includes an additional uncertainty from the MRIO analyses, which was  
376 estimated to be 13.0% according to previous studies.<sup>22,43,44</sup> These uncertainties are  
377 derived from knowledge gaps in economic statistics, sectoral mapping and data  
378 harmonization.<sup>45,46</sup> The simulation of the atmospheric chemical transport model is subject

379 to errors in emission inputs and the model representation of tropospheric physical and  
380 chemical processes. However, performing Monte Carlo and other sensitivity simulations  
381 that require high computational costs is computationally prohibitive. Instead, we use the  
382 normalized root-mean-square deviation (NRMSD) between the simulated and observed  
383 results of atmospheric deposition to represent the uncertainties on the model in terms of  
384 the method presented in Zhang et al.<sup>44</sup> Based on the method and the model evaluations in  
385 our previous work,<sup>28</sup> the NRMSD is estimated to be 23.1% for atmospheric Hg  
386 simulation over the model domain in 2010. In summary, based on the aggregation of the  
387 uncertainties above, we estimate an overall uncertainty of [-34.1%, 37.1%] for  
388 atmospheric deposition and outflow in Section 3.1 and [-36.4%, 39.3%] for changes in  
389 atmospheric deposition and outflow in Section 3.2.

390 The MRIO database used in this study is derived from Liu et al.,<sup>29</sup> while many other  
391 MRIO databases have been developed for China, such as those developed by Shi and  
392 Zhang,<sup>47</sup> Zhang and Qi,<sup>48</sup> and Wang et al.<sup>49,50</sup> Especially, Wang et al.<sup>49,50</sup> have recently  
393 developed a more resolution-detailed and time-detailed MRIO database for China, which  
394 also comes with accompanying standard deviation tables. The use of the database from  
395 Liu et al.<sup>29</sup> makes it easy to compare our results to those of most previous studies that  
396 used the database, and it will be critical and possible to compare and harmonize the  
397 results based on the other databases in future studies. Meanwhile, to evaluate the impacts  
398 of interprovincial trade on atmospheric deposition over neighboring regions, we choose  
399 several representative neighboring seas and lands but do not include all neighboring  
400 regions of China in this study. Through additional measurements and models of the  
401 marine Hg cycle and diet habits of humans, the evaluation of human MeHg exposure

402 risks from the consumption of seafood harvested from marine regions outside the eastern  
403 terrestrial boundary of China would assist further analysis of this subject in the future.  
404 Moreover, transboundary Hg pollution has interactional impacts between China and  
405 neighboring countries. We investigate the impacts of Chinese emissions on neighboring  
406 countries from the perspective of interprovincial trade in this study. The impacts of  
407 emissions from neighboring countries on China need to be studied from the perspective  
408 of international trade in the future.

409 **Author Information**

410 **Corresponding Authors**

411 \*(J.S.) Phone: +86-21-54341198; e-mail: jshu@geo.ecnu.edu.cn.

412 \*(X.W.) Phone: +86-10-62759190; e-mail: xjwang@urban.pku.edu.cn.

413

414 **Acknowledgments**

415 The authors would like to thank the editor and anonymous reviewers for their thoughtful  
416 comments. This study was funded by the National Natural Science Foundation of China  
417 (41701589, 41630748, 41271055), and China Postdoctoral Science Foundation Grant  
418 (2017M611492, 2018T110372). Sai Liang thanks the financial support of the  
419 Fundamental Research Funds for the Central Universities and Interdiscipline Research  
420 Funds of Beijing Normal University. All map images are plotted by GAMAP (Global  
421 Atmospheric Model Analysis Package, Version 2.17;  
422 <http://acmg.seas.harvard.edu/gamap/>). The computation was supported by the High  
423 Performance Computer Center of East China Normal University.

424

425 **Supporting Information**

426 Additional information on study domain and boundaries for regional definitions (Figure  
427 S1; Dataset S1), net emission flows induced by interprovincial trade in 2010 (Figure S2),  
428 seasonal distribution of wind speed and wind direction over East Asian domain in 2010  
429 (Figure S3), sector classification of the Chinese MRIO table and allocation of emissions  
430 in this study (Datasets S2 and S3), provincial production-based and trade-induced  
431 emissions and associated sector-specified data in 2010 (Datasets S4 and S5).

432 **Reference**

- 433 1 Arctic Monitoring and Assessment Programme and United Nations Environment  
434 Programme (AMAP/UNEP). *Technical Background Report for the Global*  
435 *Mercury Assessment*; AMAP/UNEP: Geneva, Switzerland, 2013.
- 436 2 Corbitt, E. S.; Jacob, D. J.; Holmes, C. D.; Streets, D. G.; Sunderland, E. M.  
437 Global source-receptor relationships for mercury deposition under present-day  
438 and 2050 emissions scenarios. *Environ. Sci. Technol.* **2011**, *45* (24), 10477–  
439 10484.
- 440 3 Harris, R. C.; Rudd, J. W. M.; Amyot, M.; Babiarz, C. L.; Beaty, K. G.;  
441 Blanchfield, P. J.; Bodaly, R. A.; Branfireun, B. A.; Gilmour, C. C.; Graydon, J.  
442 A. Whole-ecosystem study shows rapid fish-mercury response to changes in  
443 mercury deposition. *Proc. Natl. Acad. Sci. U. S. A.* **2007**, *104* (42), 16586–16591.
- 444 4 Vijayaraghavan, K.; Levin, L.; Parker, L.; Yarwood, G.; Streets, D. Response of  
445 fish tissue mercury in a freshwater lake to local, regional, and global changes in  
446 mercury emissions. *Environ. Toxicol. Chem.* **2014**, *33* (6), 1238–1247.
- 447 5 Roman, H. A.; Walsh, T. L.; Coull, B. A.; Dewailly, É.; Guallar, E.; Hattis, D.;  
448 Mariën, K.; Schwartz, J.; Stern, A. H.; Virtanen, J. K. Evaluation of the  
449 cardiovascular effects of methylmercury exposures: Current evidence supports  
450 development of a dose–response function for regulatory benefits analysis.  
451 *Environ. Health Persp.* **2011**, *119* (5), 607–614.

- 452 6 Grandjean, P.; Satoh, H.; Murata, K.; Eto, K. Adverse effects of methylmercury:  
453 Environmental health research implications. *Environ. Health Persp.* **2010**, *118*  
454 (8), 1137–1145.
- 455 7 Karagas, M. R.; Choi, A. L.; Oken, E.; Horvat, M.; Schoeny, R.; Kamai, E.;  
456 Cowell, W.; Grandjean, P.; Korrick, S. Evidence on the human health effects of  
457 low-level methylmercury exposure. *Environ. Health Persp.* **2012**, *120* (6), 799–  
458 806.
- 459 8 National Institute for Minamata Disease (NIMD), Ministry of the Environment.  
460 *Minamata disease archives*, <http://www.nimd.go.jp/english/>.
- 461 9 United Nations Environment Programme (UNEP). *Minamata Convention on*  
462 *Mercury*, <http://www.mercuryconvention.org>.
- 463 10 Zhang, L.; Wang, S.; Wang, L.; Wu, Y.; Duan, L.; Wu, Q.; Wang, F.; Yang, M.;  
464 Yang, H.; Hao, J. Updated emission inventories for speciated atmospheric  
465 mercury from anthropogenic sources in China. *Environ. Sci. Technol.* **2015**, *49*  
466 (5), 3185–3194.
- 467 11 Wu, Q.; Wang, S.; Li, G.; Liang, S.; Lin, C. J.; Wang, Y.; Cai, S.; Liu, K.; Hao, J.  
468 Temporal trend and spatial distribution of speciated atmospheric mercury  
469 emissions in China during 1978–2014. *Environ. Sci. Technol.* **2016**, *50* (24),  
470 13428–13435.
- 471 12 Ogawa, S.; Okochi, H.; Ogata, H.; Umezawa, N.; Miura, K.; Kato, S. Observation  
472 of gaseous elemental mercury (GEM) in the free troposphere at Mt. Fuji: Summer

- 473           observational campaign in 2014. *J. Japan Soci. Atmos. Environ.* **2015**, *50*, 100–  
474           106.
- 475    13    Nagafuchi, O.; Yokota, K.; Kato, S.; Osaka, K. I.; Nakazawa, K.; Koga, M.;  
476           Hishida, N.; Nishida, Y. Origin of atmospheric gaseous mercury using the Hg/CO  
477           ratio in pollution plume observed at Mt. Fuji Weather Station; *Japan Geoscience*  
478           *Union Meeting 2014*: Pacifico Yokohama, Kanagawa, Japan, 28 April–02 May  
479           2014.
- 480    14    Jaffe, D.; Prestbo, E.; Swartzendruber, P.; Weiss-Penzias, P.; Kato, S.; Takami,  
481           A.; Hatakeyama, S.; Kajii, Y. Export of atmospheric mercury from Asia. *Atmos.*  
482           *Environ.* **2005**, *39* (17), 3029–3038.
- 483    15    Sprovieri, F.; Pirrone, N.; Ebinghaus, R.; Kock, H.; Dommergue, A. A review of  
484           worldwide atmospheric mercury measurements. *Atmos. Chem. Phys.* **2010**, *10*,  
485           8245–8265.
- 486    16    Lin, C. J.; Pan, L.; Streets, D. G.; Shetty, S. K.; Jang, C.; Feng, X.; Chu, H. W.;  
487           Ho, T. C. Estimating mercury emission outflow from East Asia using CMAQ-Hg.  
488           *Atmos. Chem. Phys.* **2010**, *10* (4), 1853–1864.
- 489    17    Pan, L.; Lin, C. J.; Carmichael, G. R.; Streets, D. G.; Tang, Y.; Woo, J. H.;  
490           Shetty, S. K.; Chu, H. W.; Ho, T. C.; Friedli, H. R. Study of atmospheric mercury  
491           budget in East Asia using STEM-Hg modeling system. *Sci. Total Environ.* **2010**,  
492           *408* (16), 3277–3291.
- 493    18    Chen, L.; Wang, H. H.; Liu, J. F.; Tong, Y. D.; Ou, L. B.; Zhang, W.; Hu, D.;  
494           Chen, C.; Wang, X. J. Intercontinental transport and deposition patterns of



- 495 atmospheric mercury from anthropogenic emissions. *Atmos. Chem. Phys.* **2014**,  
496 *13* (9), 25185–25218.
- 497 19 Durnford, D.; Dastoor, A.; Figueras-Nieto, D.; Ryjkov, A. Long range transport  
498 of mercury to the Arctic and across Canada. *Atmos. Chem. Phys.* **2010**, *10*, 6063–  
499 6086.
- 500 20 Pirrone, N.; Keating, T. *Hemispheric Transport of Air Pollution 2010, Part B:*  
501 *Mercury*; United Nations Publication: Geneva, Switzerland, 2011.
- 502 21 Wang, H.; Zhang, Y.; Zhao, H.; Lu, X.; Zhang, Y.; Zhu, W.; Nielsen, C. P.; Li,  
503 X.; Zhang, Q.; Bi, J. Trade-driven relocation of air pollution and health impacts in  
504 China. *Nat. Commun.* **2017**, *8* (1), 738.
- 505 22 Peters, G. P.; Davis, S. J.; Andrew, R. A synthesis of carbon in international trade.  
506 *Biogeosciences* **2012**, *9*, 3247–3276.
- 507 23 Feng, K.; Davis, S. J.; Sun, L.; Li, X.; Guan, D.; Liu, W.; Liu, Z.; Hubacek, K.  
508 Outsourcing CO<sub>2</sub> within China. *Proc. Natl. Acad. Sci. U. S. A.* **2013**, *110* (28),  
509 11654–11659.
- 510 24 Hui, M.; Wu, Q.; Wang, S.; Liang, S.; Zhang, L.; Wang, F.; Lenzen, M.; Wang,  
511 Y.; Xu, L.; Lin, Z. Mercury flows in China and global drivers. *Environ. Sci.*  
512 *Technol.* **2017**, *51* (1), 222–231.
- 513 25 Liang, S.; Xu, M.; Liu, Z.; Suh, S.; Zhang, T. Socioeconomic drivers of mercury  
514 emissions in China from 1992 to 2007. *Environ. Sci. Technol.* **2013**, *47* (7), 3234–  
515 3240.

- 516 26 Liang, S.; Chao, Z.; Wang, Y.; Ming, X.; Liu, W. Virtual atmospheric mercury  
517 emission network in China. *Environ. Sci. Technol.* **2014**, *48* (5), 2807–2815.
- 518 27 Li, J. S.; Chen, G. Q.; Chen, B.; Yang, Q.; Wei, W. D.; Wang, P.; Dong, K. Q.;  
519 Chen, H. P. The impact of trade on fuel-related mercury emissions in Beijing–  
520 evidence from three-scale input-output analysis. *Renew. Sust. Energ. Rev.* **2017**,  
521 *75*, 742–752.
- 522 28 Chen, L.; Meng, J.; Liang, S.; Zhang, H.; Zhang, W.; Liu, M.; Tong, Y.; Wang,  
523 H.; Wang, W.; Wang, X.; Shu, J. Trade-induced atmospheric mercury deposition  
524 over China and implications for demand-side controls. *Environ. Sci. Technol.*  
525 **2018**, *52* (4), 2036–2045.
- 526 29 Liu, W. D.; Tang, Z. P.; Chen, J.; Yang, B. *China's interregional input–output*  
527 *table for 30 regions in 2010 (in Chinese)*; China Statistics Press: Beijing, China,  
528 2014.
- 529 30 Peters, G. P.; Weber, C. L.; Guan, D.; Hubacek, K. China's growing CO<sub>2</sub>  
530 emissions—a race between increasing consumption and efficiency gains. *Environ.*  
531 *Sci. Technol.* **2007**, *41* (17), 5939–5944.
- 532 31 Weber, C. L.; Peters, G. P.; Guan, D.; Hubacek, K. The contribution of Chinese  
533 exports to climate change. *Energy Policy* **2008**, *36* (9), 3572–3577.
- 534 32 Selin, N. E.; Jacob, D. J.; Park, R. J.; Yantosca, R. M.; Strode, S.; Jaeglé, L.;  
535 Jaffe, D. Chemical cycling and deposition of atmospheric mercury: Global  
536 constraints from observations. *J. Geophys. Res. Atmos.* **2007**, *112* (D2), 557–573.

- 537 33 Holmes, C. D.; Jacob, D. J.; Corbitt, E. S.; Mao, J.; Yang, X.; Talbot, R.; Slemr,  
538 F. Global atmospheric model for mercury including oxidation by bromine atoms.  
539 *Atmos. Chem. Phys.* **2010**, *10* (24), 12037–12057.
- 540 34 Soerensen, A. L.; Sunderland, E. M.; Holmes, C. D.; Jacob, D. J.; Yantosca, R.  
541 M.; Skov, H.; Christensen, J. H.; Strode, S. A.; Mason, R. P. An improved global  
542 model for air-sea exchange of mercury: High concentrations over the North  
543 Atlantic. *Environ. Sci. Technol.* **2010**, *44* (22), 8574–8580.
- 544 35 Amos, H. M.; Jacob, D. J.; Holmes, C. D.; Fisher, J. A.; Wang, Q.; Yantosca, R.  
545 M.; Corbitt, E. S.; Galarneau, E.; Rutter, A. P.; Gustin, M. S.; Steffen, A.;  
546 Schauer, J. J.; Graydon, J. A.; Louis, V. L. S.; Talbot, R. W.; Edgerton, E. S.;  
547 Zhang, Y.; Sunderland, E. M. Gas-particle partitioning of atmospheric Hg(II) and  
548 its effect on global mercury deposition. *Atmos. Chem. Phys.* **2012**, *12* (1), 591–  
549 603.
- 550 36 Wesely, M. L. Parameterization of surface resistances to gaseous dry deposition  
551 in regional-scale numerical models. *Atmos. Environ.* **1989**, *23*, 1293–1304.
- 552 37 Liu, H.; Jacob, D. J.; Bey, I.; Yantosca, R. M. Constraints from  $^{210}\text{Pb}$  and  $^7\text{Be}$  on  
553 wet deposition and transport in a global three-dimensional chemical tracer model  
554 driven by assimilated meteorological fields. *J. Geophys. Res. Atmos.* **2001**, *106*,  
555 12109–12128.
- 556 38 Mergler, D.; Anderson, H. A.; Chan, L. H. M.; Mahaffey, K. R.; Murray, M.;  
557 Sakamoto, M.; Stern, A. H. Methylmercury exposure and health effects in  
558 humans: A worldwide concern. *Ambio* **2007**, *36* (1), 3–11.

- 559 39 Selin, N. E.; Sunderland, E. M.; Knightes, C. D.; Mason, R. P. Sources of  
560 mercury exposure for U.S. seafood consumers: Implications for policy. *Environ.*  
561 *Health Persp.* **2010**, *118*, 137–143.
- 562 40 Mahaffey, K. R.; Sunderland, E. M.; Chan, H. M.; Choi, A. L.; Grandjean, P.;  
563 Mariën, K.; Oken, E.; Sakamoto, M.; Schoeny, R.; Weihe, P.; Yan, C.-H.;  
564 Yasutake, A. Balancing the benefits of n-3 polyunsaturated fatty acids and the  
565 risks of methylmercury exposure from fish consumption. *Nut. Rev.* **2011**, *69* (9),  
566 493–508.
- 567 41 Sunderland, E. M. Mercury exposure from domestic and imported estuarine and  
568 marine fish in the U.S. seafood market. *Environ. Health Persp.* **2007**, *115*, 235–  
569 242.
- 570 42 Sunderland, E. M.; Mason, R. P. Human impacts on open ocean mercury  
571 concentrations. *Global Biogeochem. Cy.* **2007**, *21*, 177–180.
- 572 43 Lin, J.; Tong, D.; Davis, S.; Ni, R.; Tan, X.; Pan, D.; Zhao, H.; Lu, Z.; Streets, D.;  
573 Feng, T.; Zhang, Q.; Yan, Y.; Hu, Y.; Li, J.; Liu, Z.; Jiang, X.; Geng, G.; He, K.;  
574 Huang, Y.; Guan, D. Global climate forcing of aerosols embodied in international  
575 trade. *Nat. Geosci.* **2016**, *9* (10), 790–794.
- 576 44 Zhang, Q.; Jiang, X.; Tong, D.; Davis, S. J.; Zhao, H.; Geng, G.; Feng, T.; Zheng,  
577 B.; Lu, Z.; Streets, D. G.; Ni, R.; Brauer, M.; Donkelaar, A. V.; Martin, R. V.;  
578 Huo, H.; Liu, Z.; Pan, D.; Kan, H.; Yan, Y.; Lin, J.; He, K.; Guan, D.  
579 Transboundary health impacts of transported global air pollution and international  
580 trade. *Nature* **2017**, *543* (7647), 705.

- 581 45 Lenzen, M.; Moran, D.; Kanemoto, K.; Foran, B.; Lobefaro, L.; Geschke, A.  
582 International trade drives biodiversity threats in developing nations. *Nature* **2012**,  
583 *486* (7401), 109–112.
- 584 46 Steenolsen, K.; Owen, A.; Barrett, J.; Guan, D.; Hertwich, E. G.; Lenzen, M.;  
585 Wiedmann, T. Accounting for value added embodied in trade and consumption:  
586 An intercomparison of global multiregional input–output databases. *Econ. Syst.*  
587 *Res.* **2016**, *28* (1), 78–94.
- 588 47 Shi, J.; Zhang, Z. *Inter-province input-output model and interregional economic*  
589 *linkage in China (in Chinese)*; Science Press: Beijing, China, 2012.
- 590 48 Zhang, Y.; Qi, S. *China multi-regional input-output models(in Chinese)*; China  
591 Statistics Press: Beijing, China, 2012.
- 592 49 Wang, Y.; Geschke, A.; Lenzen, M. Constructing a time series of nested  
593 multiregion input-output tables. *Int. Reg. Sci. Rev.* **2017**, *40* (5), 476–499.
- 594 50 Wang, Y. An industrial ecology virtual framework for policy making in China.  
595 *Econ. Syst. Res.* **2017**, *29* (2), 252–274.
- 596

1 **Figure Captions**

2

3 **Figure 1.** Spatial distribution of atmospheric Hg deposition over East Asia driven by  
4 Chinese anthropogenic emissions (a) and the Hg mass budget for China (b). The season  
5 “winter” includes December (D), January (J), and February (F). The season “spring”  
6 includes March (M), April (A), and May (M). The season “summer” includes June (J),  
7 July (J), and August (A). The season “autumn” includes September (S), October (O), and  
8 November (N). The mass budget includes atmospheric emissions, atmospheric deposition,  
9 atmospheric burden, and atmospheric outflow.

10

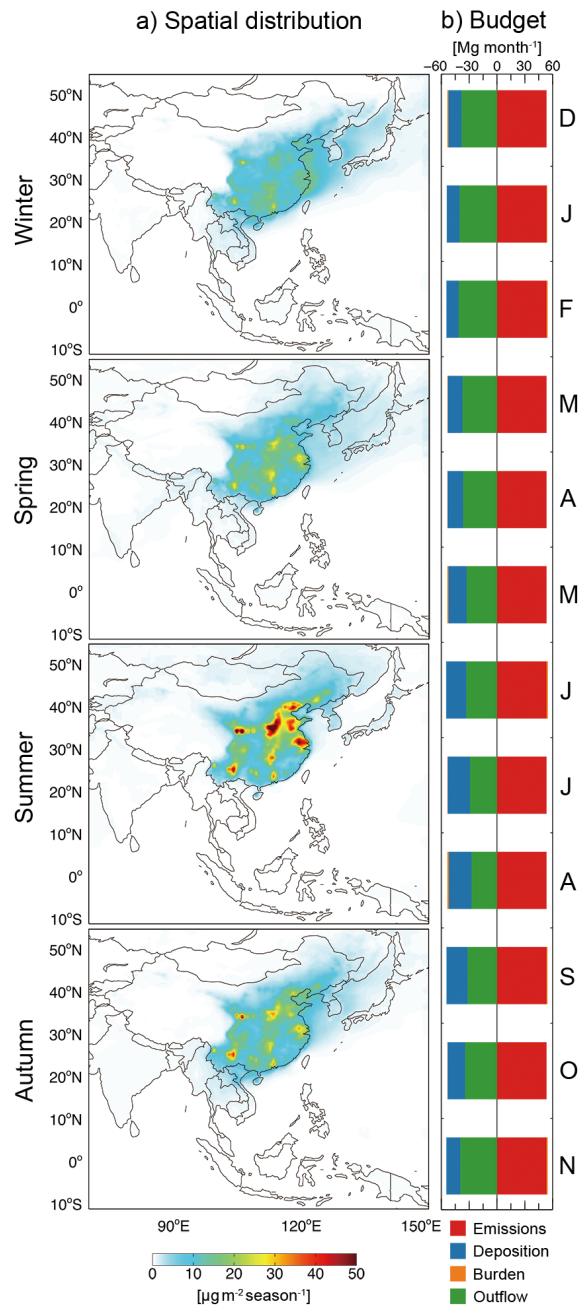
11 **Figure 2.** Changes in the spatial distribution of atmospheric Hg deposition over East Asia  
12 (a) and changes in the Hg mass budget for China (b) as driven by Chinese interprovincial  
13 trade.

14

15 **Figure 3.** Changes in the spatial distribution of atmospheric Hg deposition over East Asia  
16 except for terrestrial China as driven by Chinese interprovincial trade. The definitions of  
17 the seasons are the same as those for Figure 1. The number in blue color located in the  
18 lower left corner of each panel indicates the sum of decreasing global atmospheric  
19 deposition driven by Chinese interprovincial trade (unit: Mg season<sup>-1</sup>), and the number in  
20 red color indicates the sum of increasing global atmospheric deposition driven by  
21 Chinese interprovincial trade (unit: Mg season<sup>-1</sup>).

22

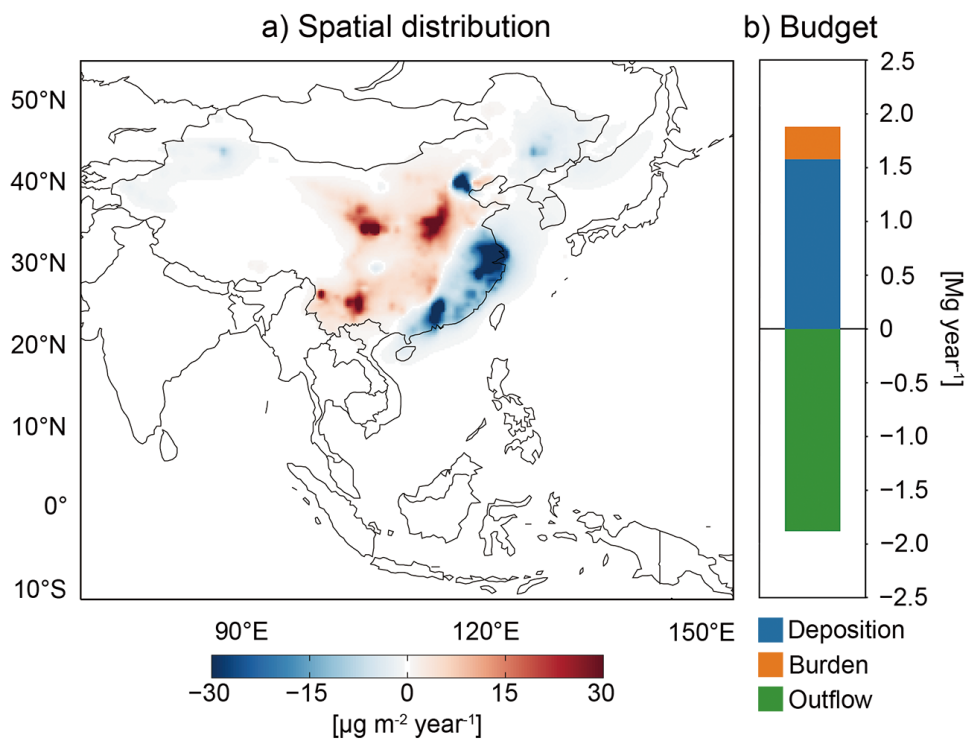
23 **Figure 4.** Changes in the atmospheric Hg budget for China and the atmospheric Hg  
24 deposition over neighboring seas and lands driven by trade-induced emissions of China.  
25 The total national anthropogenic emissions consist of emissions from each province,  
26 including the emissions embodied in the consumption of local goods, consumption of  
27 imported goods and other emissions (e.g., residential coal consumption and the use of  
28 Hg-added products). The “net” emissions represent the emissions embodied in net  
29 interprovincial trade. The unit of all the numbers except numbers in parentheses is Mg  
30 year<sup>-1</sup>. The numbers in parentheses represent the proportion of the change induced by  
31 interprovincial trade to total deposition of Chinese anthropogenic Hg over each  
32 neighboring region. The definition of each neighboring region is described in *SI Dataset*  
33 *SI*, and the Chinese coastal seas include the Bohai Sea, Yellow Sea, East China Sea, and  
34 South China Sea.  
35



36

37 **Figure 1.** Spatial distribution of atmospheric Hg deposition over East Asia driven by  
 38 Chinese anthropogenic emissions (a) and the Hg mass budget for China (b). The season  
 39 “winter” includes December (D), January (J), and February (F). The season “spring”  
 40 includes March (M), April (A), and May (M). The season “summer” includes June (J),  
 41 July (J), and August (A). The season “autumn” includes September (S), October (O), and  
 42 November (N). The mass budget includes atmospheric emissions, atmospheric deposition,  
 43 atmospheric burden, and atmospheric outflow.



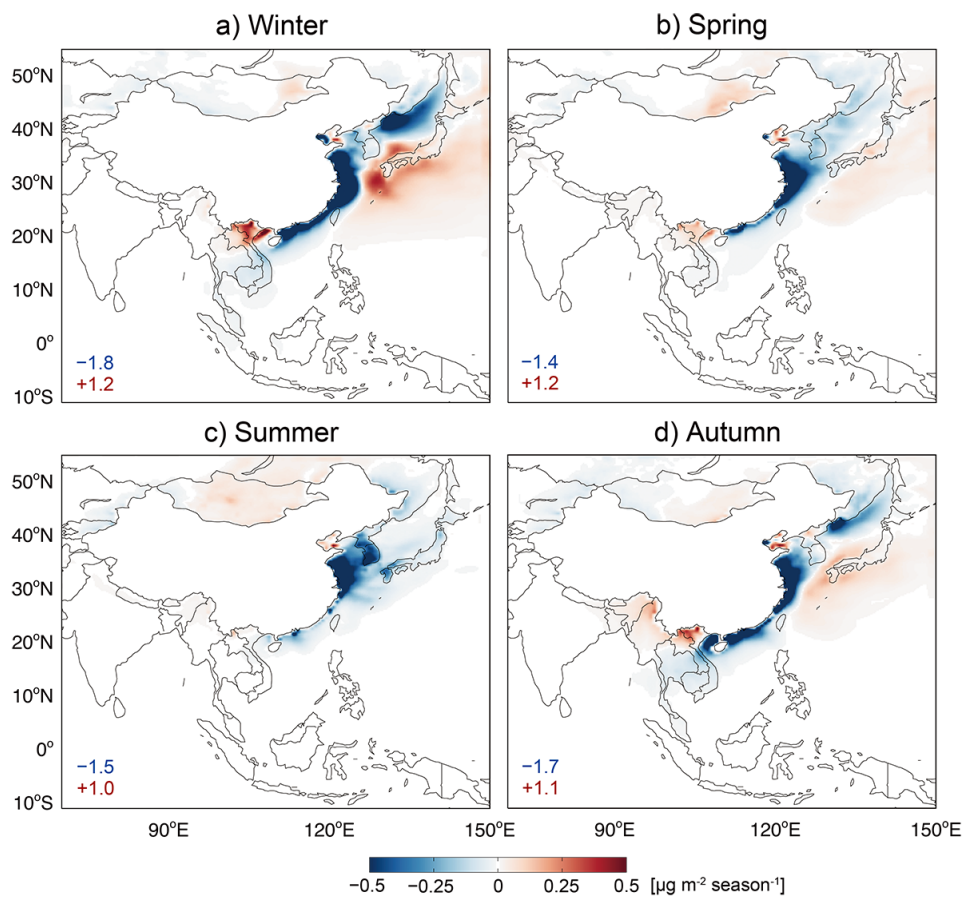


44

45 **Figure 2.** Changes in the spatial distribution of atmospheric Hg deposition over East Asia

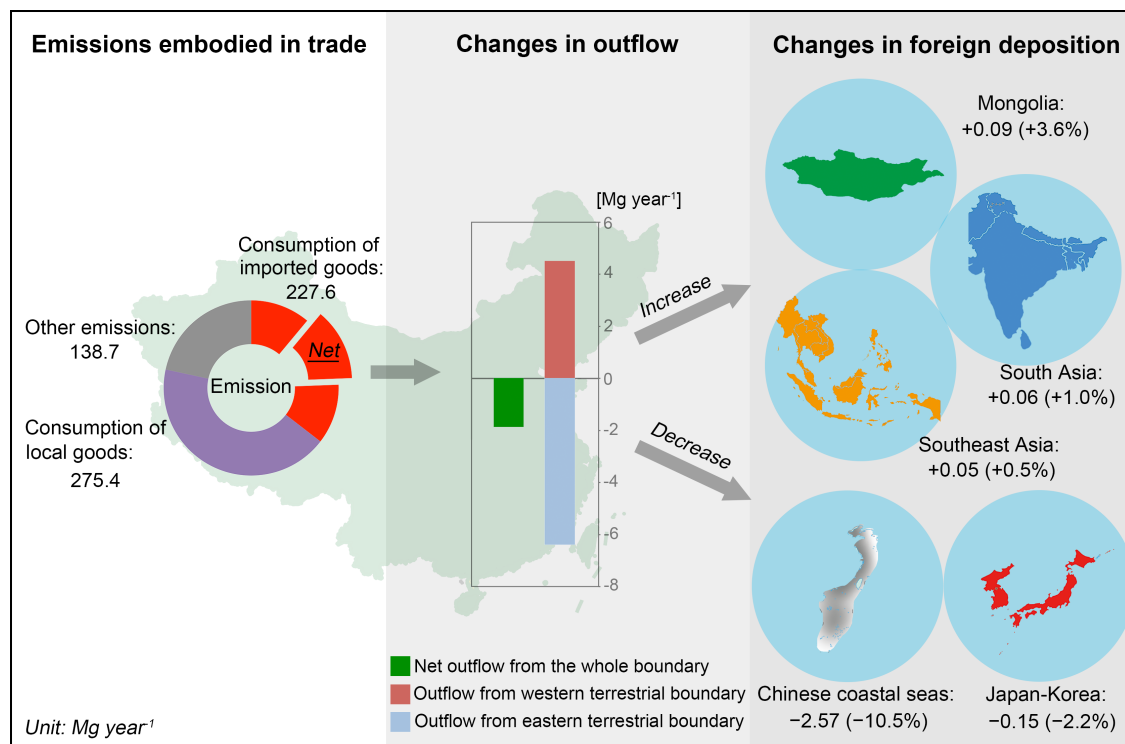
46 (a) and changes in the Hg mass budget for China (b) as driven by Chinese interprovincial

47 trade.



48

49 **Figure 3.** Changes in the spatial distribution of atmospheric Hg deposition over East Asia  
50 except for terrestrial China as driven by Chinese interprovincial trade. The definitions of  
51 the seasons are the same as those for Figure 1. The number in blue color located in the  
52 lower left corner of each panel indicates the sum of decreasing global atmospheric  
53 deposition driven by Chinese interprovincial trade (unit:  $\text{Mg season}^{-1}$ ), and the number in  
54 red color indicates the sum of increasing global atmospheric deposition driven by  
55 Chinese interprovincial trade (unit:  $\text{Mg season}^{-1}$ ).



56

57 **Figure 4.** Changes in the atmospheric Hg budget for China and the atmospheric Hg

58 deposition over neighboring seas and lands driven by trade-induced emissions of China.

59 The total national anthropogenic emissions consist of emissions from each province,

60 including the emissions embodied in the consumption of local goods, consumption of

61 imported goods and other emissions (e.g., residential coal consumption and the use of

62 Hg-added products). The “net” emissions represent the emissions embodied in net

63 interprovincial trade. The unit of all the numbers except numbers in parentheses is Mg

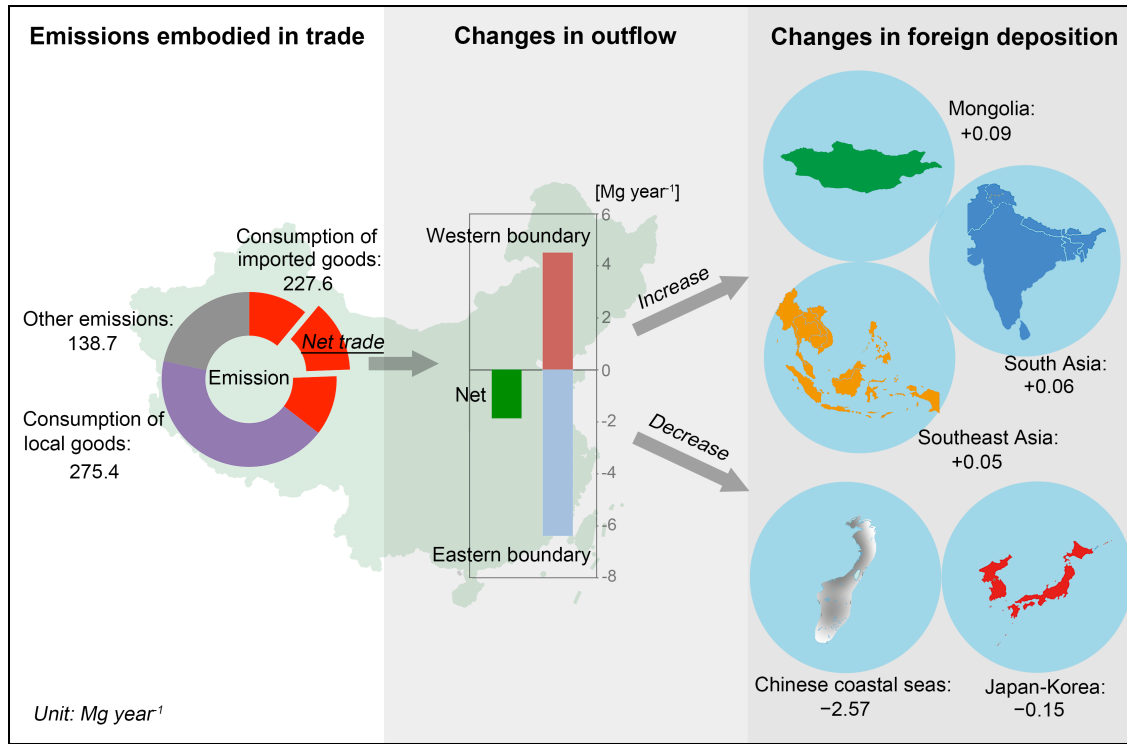
64 year<sup>-1</sup>. The numbers in parentheses represent the proportion of the change induced by

65 interprovincial trade to total deposition of Chinese anthropogenic Hg over each

66 neighboring region. The definition of each neighboring region is described in *SI Dataset*67 *SI*, and the Chinese coastal seas include the Bohai Sea, Yellow Sea, East China Sea, and

68 South China Sea.

69 TOC/Abstract Art



70